2022 EAGE ANNUAL
83RD CONFERENCE & EXHIBITION
MADRID I SPAIN

SURFACE SEISMIC WITH DAS USING OMNIDIRECTIONAL CABLE: A MODELING STUDY

A. Egorov[1], M. Charara[1], E. Alfataierge[2], A. Bakulin[2], R. Pevzner[3]

[1] Aramco Research Center; [2] EXPEC Advanced Research Center, Saudi Aramco; [3] Curtin University

Summary

Distributed acoustic sensing (DAS) systems measure smoothed strain along the cable, different from the physical quantities measured by the traditional sensors, such as geophones and hydrophones. To make progress in surface seismic with DAS systems, their realistic response needs to be modeled, understood, and taken into account during survey design. We present an algorithm to model DAS data for survey design purposes and generate realistic seismic gathers for DAS and geophone sensors in a complex near-surface model. We then analyze the characteristic properties of straight and helical DAS cables and compare them to the more traditional point geophone sensors in terms of recording the near-surface reflections and guided waves.

Surface seismic with DAS using omnidirectional cable: a modeling study

Introduction

Distributed Acoustic Sensing (DAS) systems provide measurements that are different from conventional seismic sensors, such as geophones. DAS systems measure strain or strain rate along the fiber optic cable (Parker et al., 2014). It is intuitively clear that such systems with straight surface fiber-optic cables are similar to geophones along the cable axis (horizontal in this case) and not sensitive to the P-waves traveling perpendicular to the fiber. When DAS is used for vertical seismic profiles (Mateeva et al., 2014), its directivity is similar to vertical geophones, ideal for reflection P-wave imaging. If we consider acquiring surface seismic with DAS, the cables need to be buried below the surface or are placed on the surface. In such a case, the P-waves traveling normal to the fiber (the reflected P-waves) are the primary source of information. In order to improve the sensitivity to these waves, shaped fibers were proposed, e.g., helical cables (Kuvshinov, 2016). Shaped fibers are sensitive to a weighted sum of several strain tensor components (Eaid et al., 2020) – as a result, they have different directivity characteristics, which depend on the chosen fiber shape, helical shapes having a higher sensitivity to broadside P-waves. Field datasets acquired with such sensors prove this (Tertyshnikov et al., 2020). In addition, they suggest a strong seasonal variation of such sensitivity.

For DAS systems to be applied for surface seismic acquisition, their directivity and other properties must be comprehensively understood and considered during survey design. With shaped fibers taken into account, there are quite a few parameters to consider during the survey design process: gauge length, pulse width, depth of the fiber cable, and multiple properties determining the shape of the fiber (e.g., wrapping angle for helical shapes). We outline the characteristic properties of a modeling algorithm specifically created for DAS survey design. Using this algorithm, we model several surface seismic scenarios for different distributed sensors and analyze the characteristic properties of straight and helical DAS cables compared with the more traditional particle velocity sensors.

Method

We apply a pseudospectral modeling engine to solve the elastic wave equation (Fornberg, 1987). For accurate modeling of free surface effects, we use the image condition for the free surface (Levander, 1988). Furthermore, as pseudospectral modeling allows for relatively large finite-difference grid sizes, we employ an accurate source and receiver interpolation method by Hicks (2002). This also has the additional advantage of convenient modeling of dense DAS data.

We model the response of DAS systems as the smoothed component of the strain tensor tangential to the fiber direction (Eaid et al., 2020). At each point s on the fiber, the tangential component of the strain tensor can be expressed as follows:

$$\varepsilon_{tt}(s) = (\hat{\mathbf{t}}\cdot\hat{\mathbf{x}})^2\varepsilon_{xx} + (\hat{\mathbf{t}}\cdot\hat{\mathbf{y}})^2\varepsilon_{yy} + (\hat{\mathbf{t}}\cdot\hat{\mathbf{z}})^2\varepsilon_{zz} + 2(\hat{\mathbf{t}}\cdot\hat{\mathbf{x}})(\hat{\mathbf{t}}\cdot\hat{\mathbf{y}})\varepsilon_{xy} + 2(\hat{\mathbf{t}}\cdot\hat{\mathbf{y}})(\hat{\mathbf{t}}\cdot\hat{\mathbf{z}})\varepsilon_{yz} + \\ +2(\hat{\mathbf{t}}\cdot\hat{\mathbf{x}})(\hat{\mathbf{t}}\cdot\hat{\mathbf{z}})\varepsilon_{xz} \quad (1)$$

Here, $\hat{\mathbf{t}}$ is the tangent vector to the fiber at s and $(\hat{\mathbf{x}}, \hat{\mathbf{y}}, \hat{\mathbf{z}})$ is the used Cartesian coordinate system. The DAS response can be modeled by smoothing ε_{tt} with a symmetric rectangular window with a length equal to gauge length. Eaid et al. (2020) show that the computation of DAS response can be reduced to the weighted summation of strain tensor components for shaped fibers. We use a similar algorithm, applying additional modifications to take into account the gauge length smoothing effects of DAS systems (Egorov et al., 2021).

Results

Figure 1 shows the seismic gathers modeled in a 1D near-surface model from the area identified for further field trials (V_P shown in Figure 1a). Here, we use the wrapping angle terminology opposite to Kuvshinov (2016), so the straight cable in our case corresponds to the wrapping angle of 0°. There are more and more wraps in the fiber with the increasing angle. In this example, the modeling does not

include the free surface, so the slow events are the source-generated S-waves (the source we use is vertical force). As a result, one can observe reflections on the vertical geophone recording (blue arrows Figure 1b). Qualitatively, out of the DAS gathers, no reflections can be seen for the straight cable and only hints for the 30˚ cable. For the 60˚ cable, the reflections are comparable to those observed on the geophone gather. The theoretical directivities of these cables for the incident P-waves shown in Figure 2 (where 90 degrees is the normal incidence) explain reflection strength in the modeled gathers.

We also observe a reduction in the energy of source-generated S-waves (compare Figure 1b and e), which may occur due to the DAS array and/or weighting of the strain tensor components, which favors P-waves over S-waves. This can be verified by analyzing the normalized FK spectra for these gathers shown in Figure 3. Notches caused by gauge length filtering change their locations with the increase of the winding angle that reduces effective DAS sensor length. As a result, notches interact with the direct S-wave for straight and 30˚ cables at 40 and 50 Hz, respectively. For 60˚ cable, the gauge length attenuates only higher frequencies of the direct S-wave, so its fading in Figure 1e for the low frequencies is not caused by the gauge length effect. It is important to note that the notches for 60˚ cable do not impact the reflected wavefield. This Figure also demonstrates that the 1 m spacing used here (typical for DAS systems) allows for unaliased recording of slower S-waves and surface waves, facilitating their suppression. We conclude that shaped fiber becomes sensitive to vertical P-waves and allows for additional suppression of slow events, making it particularly attractive for Weathering Reflection Survey (WRS) (Martin et al., 2009) and other shallow High-Definition near-surface surveys.

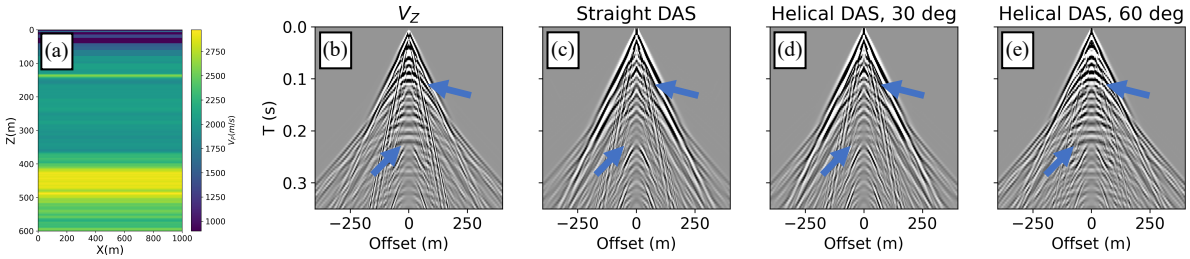

Figure 1 *Seismic gathers for the near-surface model (a) for vertical particle velocity sensor (b), straight horizontal DAS (c), helical DAS with 30˚(d) and 60˚ (e) wrapping angles. Channel spacing is 1.0 m on all gathers. All DAS gathers have a 10 m gauge length. However, the actual surface length of the single distributed channel is 10 m for (c), 8.5 m for (d), and 5 m for (e).*

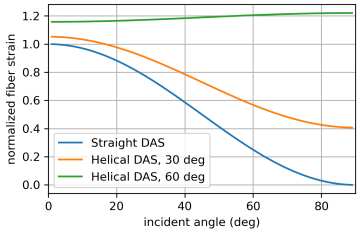

Figure 2 *Fiber directivity computed for different wrapping angles following Kuvshinov (2016) theoretical model, perfectly coupled cable.*

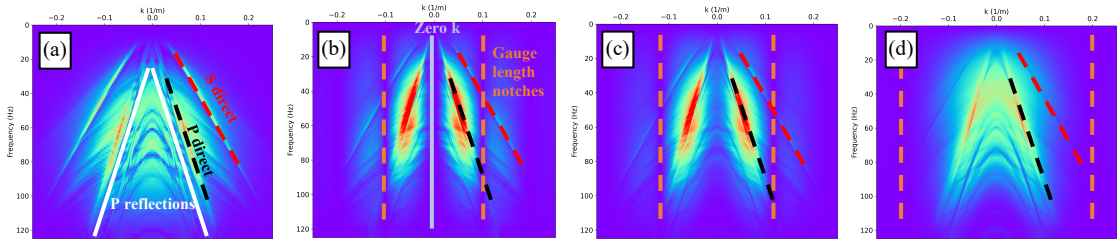

Figure 3 *FK spectra for seismic gathers from Figure 1 for vertical particle velocity sensor (a), straight horizontal DAS (b), helical DAS with 30˚(c), and 60˚(d) wrapping angles. Observe low amplitude of reflections for straight and 30˚ cable caused by directivity pattern from Figure 2.*

For the second example, we use a benchmark model by Roth and Holliger (1999) (model 3 in their paper, properties provided in Table 1). This model is a layer on a halfspace with the free surface

explicitly modeled. Again our objective here would be to sample complex near-surface arrivals properly. First, it may help us remove them in processing; second, those arrivals may be used in high-resolution elastic inversion for the near surface.

Table 1 *Subsurface benchmark model used.*

	V_P (m/s)	V_S (m/s)	Density (g/cm^3)	Thickness (m)
Layer 1	1100	330	1.6	20
Layer 2	1800	540	2.0	Halfspace

The seismic gathers simulated with the different seismic sensors are shown in Figure 4. All the sensors record a complex guided wavetrain but with a different amplitude sensitivity pattern for each. Figure 5 shows the velocity-frequency spectra corresponding to the gathers from Figure 4. All the sensor types capture the six branches of the guided waves. The velocity-frequency representations for DAS gathers with 20 m gauge length contain notches in the spectrum caused by DAS array filtering. In simple terms, the DAS array can be considered as a particular case of a point sensor array when the distance between sensors goes to zero (Bakulin et al., 2020). These notches are highlighted by the dashed red lines in Figures 5d, f. As noted before, the locations of the notches are different on the straight and helical DAS recording, even though both DAS gathers are modeled with the same gauge length. This is explained by variable DAS array length caused by increased fiber-to-cable ratio for helical fibers. For example, this ratio is ~1.7 for 54.7˚ cable, leading to a significantly smaller array length (~11.5 m) than 20 m for straight DAS, thus moving the notches.

Conclusions

We present a numerical modeling study aimed at seismic survey design with DAS cables. We present two sets of seismic gathers – one for analyzing the sensitivity of shaped fiber configurations to reflected waves and another one for analyzing the capability of DAS sensors to record the complexities of the guided wavefield for a benchmark model of a layer on a halfspace. The results agree with the existing analytical models regarding the sensitivity of helical cables to the reflected waves. The velocity-frequency analysis of the guided wave example shows that DAS systems can capture all guided wave modes in the benchmark model. In addition, characteristic notches in the velocity-frequency domain may appear for large gauge lengths describing DAS array filtering. The modeling suggests that DAS is a flexible tool, which can be made suitable for high-resolution near-surface seismic surveys. The ability to vary gauge length at the recorder distinguishes DAS from point sensor. It allows acquiring multi-scale data with variable sensor length using a single DAS cable and one round of shooting.

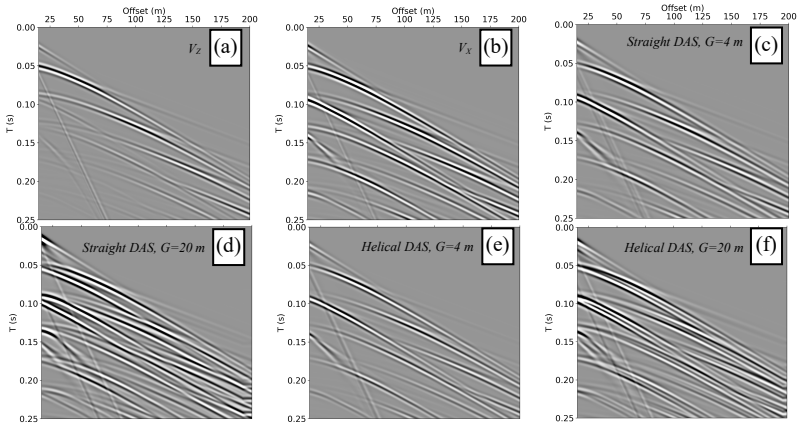

Figure 4 *Seismic gathers for the benchmark model for vertical (a) and horizontal (b) particle velocity sensors; straight DAS with gauge lengths of 4 m (c) and 20 m (d); helical DAS with 54.7˚ wrapping angle with gauge lengths of 4 m (e) and 20 m (f).*

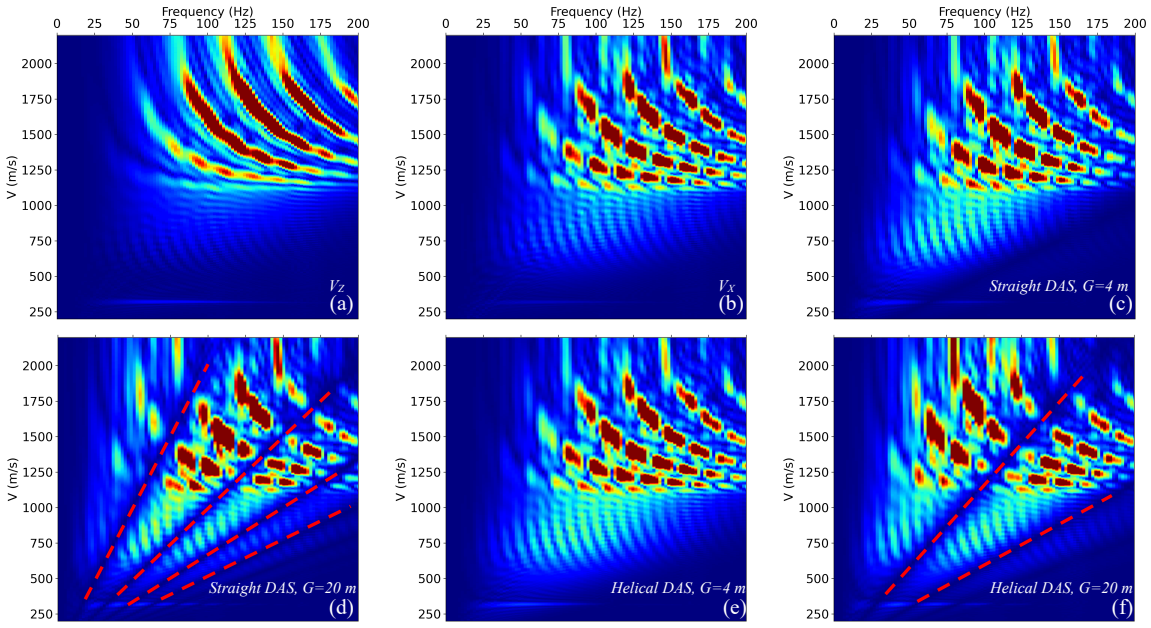

Figure 5 *A representation of the gathers from Figure 3 in the velocity-frequency domain.*

References

Bakulin, A., Silvestrov, I., and Pevzner, R. [2020]. Surface seismics with DAS: An emerging alternative to modern point-sensor acquisition. *The Leading Edge*, *39*(11), 808–818. https://doi.org/10.1190/tle39110808.1

Eaid, M. V., Keating, S. D., and Innanen, K. A. [2020]. Multiparameter seismic elastic full-waveform inversion with combined geophone and shaped fiber-optic cable data. *Geophysics*, *85*(6), R537–R552. https://doi.org/10.1190/geo2020-0170.1

Egorov, A., Charara, M., Alfataierge, E., and Bakulin, A. [2021]. *Realistic modeling of surface seismic and VSP using DAS with straight and shaped fibers of variable gauge length*. SEG/AAPG/SEPM First International Meeting for Applied Geoscience & Energy, Expanded Abstracts. https://doi.org/10.1190/segam2021-3576626.1

Fornberg, B. [1987]. The pseudospectral method: Comparisons with finite differences for the elastic wave equation. *Geophysics*, *52*(4), 483–501. https://doi.org/10.1190/1.1442319

Hicks, G. J. [2002]. Arbitrary source and receiver positioning in finite-difference schemes using Kaiser windowed sinc functions. *Geophysics*, *67*(1), 156–165. https://doi.org/10.1190/1.1451454

Kuvshinov, B. N. [2016]. Interaction of helically wound fibre-optic cables with plane seismic waves. *Geophysical Prospecting*, *64*(3), 671–688. https://doi.org/10.1111/1365-2478.12303

Levander, A. R. [1988]. Fourth-order finite-difference P-SV seismograms. *Geophysics*, *53*(11), 1425–1436. https://doi.org/10.1190/1.1442422

Martin, F., Blake, B., Colombo, C., and Elagrari, F. [2009]. Weathering reflection survey (WRS) method for statics computation in desert operations. 71st EAGE Conference and Exhibition incorporating SPE EUROPEC 2009, Extended Abstracts, cp-127.

Mateeva, A., Lopez, J., Potters, H., Mestayer, J., Cox, B., Kiyashchenko, D., Wills, P., Grandi, S., Hornman, K., Kuvshinov, B., Berlang, W., Yang, Z., and Detomo, R. [2014]. Distributed acoustic sensing for reservoir monitoring with vertical seismic profiling. *Geophysical Prospecting*, *62*(4), 679–692. https://doi.org/10.1111/1365-2478.12116

Parker, T., Shatalin, S., and Farhadiroushan, M. [2014]. Distributed Acoustic Sensing – a new tool for seismic applications. *First Break*, *32*(2), 61–69. https://doi.org/10.3997/1365-2397.2013034

Roth, M., and Holliger, K. [1999]. Inversion of source-generated noise in high-resolution seismic data. *The Leading Edge*, *18*(12), 1402–1406.

Tertyshnikov, K., Bergery, G., Freifeld, B., and Pevzner, R. [2020]. Seasonal Effects on DAS using Buried Helically Wound Cables. *EAGE Workshop on Fiber Optic Sensing for Energy Applications in Asia Pacific*, *2020*(1), 1–5. https://doi.org/10.3997/2214-4609.202070007